International Conference on Control, Engineering & Information Technology (CEIT'13)
Proceedings Engineering & Technology - Vol.3, pp. 33-38, 2013

A controlled topology for a grid connected photovoltaic system

Sihem Elhelali[1] , Noureddine Hidouri[2] , Lassâad Sbita[3]

[1]sihemelhelali@yahoo.fr, [2]noureddine.hidouri@yahoo.fr, [3]lassaad.sbita@enig.rnu.tn

Research Unit of Photovoltaic, Wind turbine and Geothermal Systems

National Engineering School of Gabes, Tunisia

***Abstract*—in this paper, the authors present a controlled topology for a grid connected photovoltaic system (GCPS). The considered system is composed of a photovoltaic array, an inverter a boost converter and a grid. The boost converter is used in order to adapt the voltage required by the PWM controlled inverter. The inverter is used to produce a three phase supply that will be connected to the grid. A filter grid, a PLL, regulators and a decoupling bloc are used in order to perform the controlled topology system.**

An extensive simulation work was performed in order to show the important results. To prove the high system performances, the presented results are discussed and illustrate how the proposed methodology is an efficient controlled topology.

***Keywords*— GCPS, inverter, boost converter, PWM, regulators.**

I. INTRODUCTION

Photovoltaic is attractive and dominant energy source, the alternative energy is characterized by its sustainability, renewability and pollution reduction [1]. It is participate in diverse applications, from the implementation study in the literature include the grid connected photovoltaic systems (GCPS) [2], [3]. The main purpose of The PV system integration to the power system is to transfer maximum solar array energy into grid with a unity power factor, this type of energy production and in order to adapt the DC voltage required by the inverter connected grid, it is necessary to use a DC-DC converter [3], [4].

This paper discusses the indirect topology of a grid connected photovoltaic system (GCPS) and the simulation of the typical structure (fig. 1). This configuration consists of a PV generator with two stages of adaptation, a boost converter and a PWM controlled inverter. A filter grid is used to reduce the ripple components due to PWM switching operation and the utility grid.

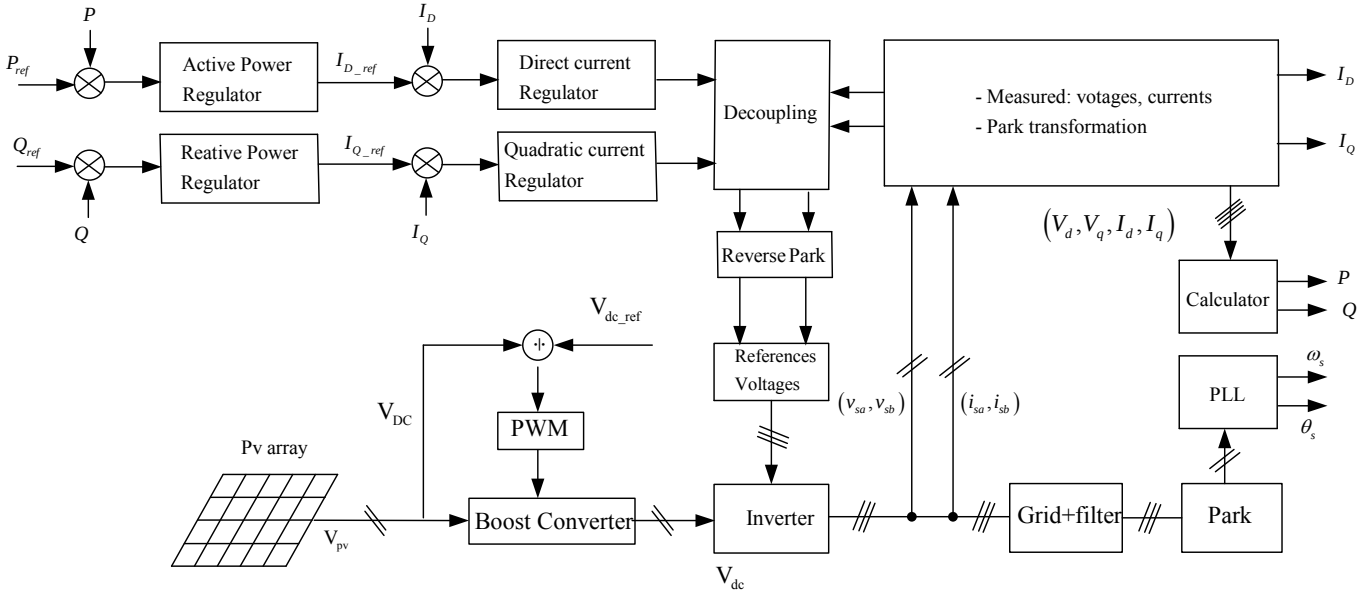

Fig.1 Proposed grid connected photovoltaic system topology

A. Cell and PV Models

Solar PV systems technologies have known an extensive research; it is an attractive source of renewable energy for distributed urban power generation [16], [17].

Solar cell is a p-n junction semiconductor, with which characteristics similar to diodes. Parameters of the solar cell are modelled as a diode in parallel with a constant current source and a shunt resistor [18]. In order to prove their research work, many authors proposed different models for the solar cell [5-7], [9]. In this work, the electric model of a solar cell is shown in fig.2, [6], [7].

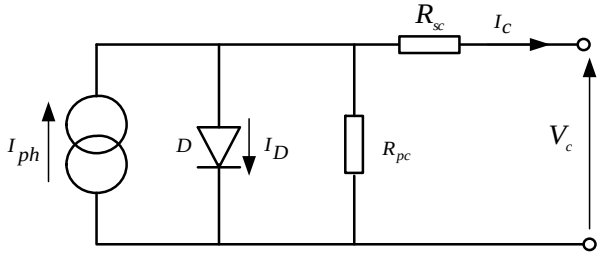

Fig. 2: Equivalent solar cell's electric circuit

The photocurrent cell I_{ph} depends on solar irradiation G and the desired cell junction temperature T_c according to equation (1), where K_{SCT} means for the short circuit current temperature coefficient and the photocurrent I_{ph_ref} is equal to the reverse saturation current I_{sc_ref} at the reference condition defined by the cell junction temperature T_{c_ref} and the insulation G_{ref} [5].

$$I_{ph} = \frac{G}{G_{ref}}\left(I_{sc\_ref} + K_{SCT}\left(T_c - T_{c\_ref}\right)\right) \qquad (1)$$

The desired reverse saturation current I_{rs} is given by relation(2), where E_g, q, k and β are indicated in table I.

$$I_{rs} = I_{rs\_ref}\left(\frac{T_c}{T_{c\_ref}}\right)\exp\left[\frac{qE_g}{\beta k}\left(\frac{1}{T_c} - \frac{1}{T_{c\_ref}}\right)\right] \qquad (2)$$

The characteristic equation of the current and voltage of a solar cell is represented by equation (3).

$$I_c = I_{ph} - I_{rs}\left(\exp\left(\frac{q}{\beta k T_c}\left(V_c + R_{sc}I_c\right) - 1\right)\right) - \frac{\left(V_c + R_{sc}I_c\right)}{R_{pc}} \qquad (3)$$

Where I_c the cell is's current, V_c is the cell's voltage.

The solar panel can be composed of N_p array of modules assembled in parallel; each one can be composed of N_s modules assembled in series. A module can also contain n_s cells associated in series configuration. This consideration expresses the relations between the panel's and the cells parameters, relation(4).

$$\begin{cases} I_p = N_p I_c \\ V_p = n_s N_s V_c \\ R_{sp} = \dfrac{n_s N_s}{N_p} R_{sc} \\ R_{pp} = \dfrac{n_s N_s}{N_p} R_{pc} \end{cases} \qquad (4)$$

In this consideration, the non-linear characteristic equation related the panel current I_p to its voltage V_p is shown in(5).

$$I_p = N_p I_{ph} - N_p I_{rs}\left(\exp\frac{q}{\beta k T_c}\left(\frac{V_p}{n_s N_s} + \frac{R_{sc}I_P}{N_p}\right) - 1\right) - \frac{N_p}{R_{pc}}\left(\frac{V_p}{n_s N_s} + \frac{R_{sc}I_P}{N_p}\right) \qquad (5)$$

B. Voltage inverter model

Fig.3 gives the general diagram of a three-phase voltage inverter. Following this configuration and in order to not shorting-circuit the supply the arm switches and their control signals must be complementary. According to this main precaution one can sufficiently use 3 Boolean variables $(c_1, c_2 \text{ and } c_3)$ to describe the inverter commands. The lower arm switch variables $(c_4, c_5 \text{ and } c_6)$ can be derived from $(c_1, c_2 \text{ and } c_3)$ as follows, [6]:

$$\begin{cases} c_4 = 1 - c_1 \\ c_5 = 1 - c_2 \\ c_6 = 1 - c_3 \end{cases} \qquad (6)$$

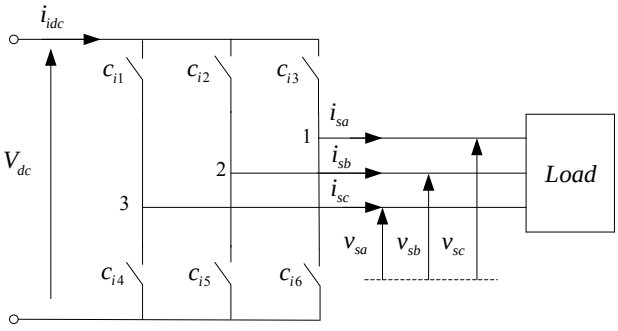

Fig. 3: Inverter-Load Configuration

In the naturel frame, the output inverter voltage can be expressed from the lower arm switch variables $(c_4, c_5 \text{ and } c_6)$ and the input voltage V_{dc} by the relation (7)

$$\begin{bmatrix} v_{sa} \\ v_{sb} \\ v_{sc} \end{bmatrix} = \frac{V_{dc}}{3} \begin{bmatrix} -2 & 1 & 1 \\ 1 & -2 & 1 \\ 1 & 1 & -2 \end{bmatrix} \begin{bmatrix} c_{i4} \\ c_{i5} \\ c_{i6} \end{bmatrix} \quad (7)$$

Another way is proposed, [8], in a fixed reference frame as the Concordia frame, to express the direct and the quadratic components of the inverter voltage, the following relation is built all around $(c_4, c_5 \text{ and } c_6)$ as Boolean variables defining the states of the inverter lower keys:

$$\bar{v} = v_d + jv_q = \sqrt{\frac{2}{3}} V_{dc} \left(c_4 e^{j\pi} + c_5 e^{j\frac{5\pi}{3}} + c_6 e^{j\frac{\pi}{3}} \right) \quad (8)$$

According to relation(8), the inverter vectors are supported by 8 vectors that can be classified in two groups; the first one is composed of two null vectors, the second is composed of 6 vectors that can be presented as a geometric progression defined by the first term $\sqrt{\frac{2}{3}} V_{dc}$ and the ratio $e^{j\frac{\pi}{3}}$. Taking those into considerations, the active vectors form a balanced voltage system; having the same module and a regular phases. Thus the inverter voltage vectors expressions are given by:

$$\begin{cases} \bar{v}_{sk} = 0 & if \quad k = 0 \ \ or \ \ k = 7 \\ \bar{v}_{sk} = q^{(k-1)} \bar{v}_{s1} \\ \bar{v}_{s1} = \sqrt{\frac{2}{3}} V_{dc} & if \quad k = 1, 2, ...6 \\ q = e^{j\frac{\pi}{3}} \end{cases} \quad (9)$$

The space representation of these vectors indicating the combination of the associated keys state $(c_4, c_5 \text{ and } c_6)$ is illustrated by fig.4.

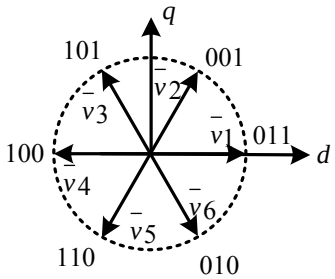

Fig. 4: Diagram of the three-phase inverter voltage vectors

C. Model of the Boost converter

The schematic of the boost converter power stage that provides a stepped-up voltage to the load is given in fig. 5.

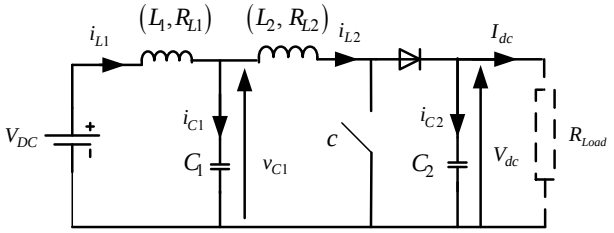

Fig. 5. Structure of the boost converter

The model of the used Boost converter is developed in [6] and reformulated in [8]; we designate by c a Boolean variable that takes the value $(c = 0)$ if the ideal key is switched off and the diode is switched on and takes the value $(c = 1)$ if the ideal key is switched on and the diode is switched off. According to this idea, the global model taking account of the boost converter model is given as, [8]:

$$\begin{bmatrix} \dot{i}_{L1} \\ \dot{i}_{L2} \\ \dot{V}_{c1} \\ \dot{V}_{c2} \end{bmatrix} = \begin{bmatrix} -\frac{R_{L1}}{L_1} & 0 & -\frac{1}{L_1} & 0 \\ 0 & -\frac{R_{L2}}{L_2} & \frac{1}{L_2} & -\frac{\bar{c}}{L_2} \\ \frac{1}{C_1} & -\frac{1}{C_1} & 0 & 0 \\ 0 & \frac{\bar{c}}{C_2} & 0 & -\frac{1}{R_{Load} C_2} \end{bmatrix} \begin{bmatrix} i_{L1} \\ i_{L2} \\ V_{C1} \\ V_{C2} \end{bmatrix} + \begin{bmatrix} \frac{1}{L_1} \\ 0 \\ 0 \\ 0 \end{bmatrix} V_{DC} \quad (10)$$

$$V_{dc} = \begin{bmatrix} 0 & 0 & 0 & 1 \end{bmatrix} \begin{bmatrix} i_{L1} & i_{L2} & V_{C1} & V_{C2} \end{bmatrix}^t \quad (11)$$

D. Model of the Grid Filter

In the Park frame, the model of the grid filter is given by relation (12) where $\bar{I}$, $\bar{V}$, $\bar{E}$, ω, R_f, L_f are respectively, the injected current in the main grid, the output inverter voltage, the grid voltage, the fundamental angular frequency, the resistance and the inductance filter.

$$\frac{d\bar{I}}{dt} = -\frac{R_f}{L_f} \bar{I} - j\omega \bar{I} + \frac{\bar{V} - \bar{E}}{L_f} \quad (12)$$

E. Model of the DC-bus

The mathematical model of the DC bus given by the equation (13) where C is the capacitance of the capacitor and I_c is the DC-bus current.

$$\frac{dV_{dc}}{dt} = CI_c \quad (13)$$

II. THE CONTROLLED SYSTEM STRATEGY

A. Regulation of grid current

The transfer function of the PI current controller is given by:

$$C_I(p) = K_p + \frac{K_I}{p} \tag{14}$$

Taking account with the filter transfer function $\frac{1}{R_f + L_f p}$,

The closed loop transfer function of the direct and the quadrature current is given by(15), where (I_{dref}, I_{qref}), (I_d, I_q) represent respectively the reference direct and quadrature currents, the measured direct and quadratic currents, [13], [14], [15].

$$H_I(p) = \frac{I_d}{I_{dref}} = \frac{I_q}{I_{qref}} = \frac{K_p p + K_I}{L_f p^2 + (K_p + K_I) p + K_I} \tag{15}$$

The standard second order system transfer function is given by relation(16).

$$H(p) = \frac{\omega_n^2}{p^2 + 2\xi\omega_n p + \omega_n^2} \tag{16}$$

Taking account with relations (15) and (16) the damping ration (ξ) and the naturel frequency (ω_n) can be expressed by (17) and (18).

$$K_p = 2\xi\omega_n L_f - R_f \tag{17}$$

$$K_I = L_f \omega_n^2 \tag{18}$$

B. PLL current synchronization references

Fig. 6 gives the schematic diagram of the will known phase looked bloc diagram based on the zero crossing voltage detection in the Concordia reference frame since $E_{dref} = 0$, [10-12].

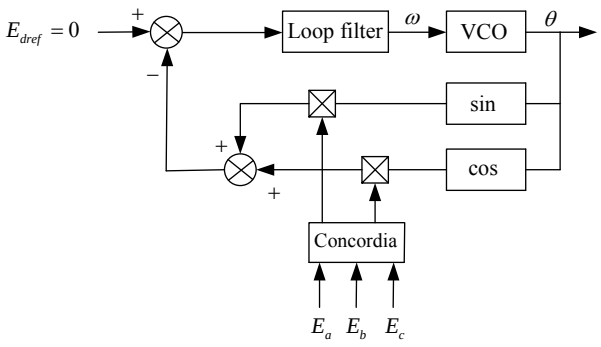

Fig. 6: Phase locked loop block diagram

The technique phase locked loop (PLL) is an important part of the control unit of a grid connected power converter. It consists in generating the desired phase for the reference current and it is based on the detection of the zero crossing of the direct component of the voltage grid. It is based on the principal of synchronous rotating frame, low-pass filter and voltage controlled oscillator (VCO), which integrates the grid frequency. The dynamic of the PLL system will set the output of the PI controller to the angular frequency reference [10-12], [19-22], this output signal is generated by the voltage controlled oscillator whose control signal is provided by a loop controller or a loop filter. PLL is simply a servo system, which controls the phase of its output signal in such a way that the error between output phase and reference phase reduces to a minimum [20], [21].

C. Regulation of the active and the reactive powers

Many authors purpose different bloc power control to regulate the active and the reactive powers, [23], [24]. Fig. 7 gives the bloc power diagram used in this research work.

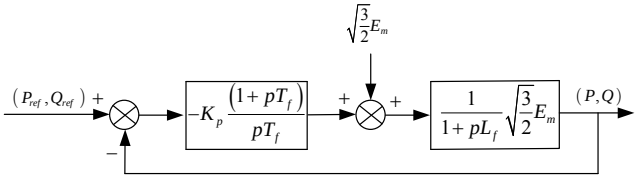

Fig. 7: Bloc power control diagram

The transfer function of the PI controller is given by:

$$\begin{cases} C(p) = K_p + \dfrac{K_I}{p} \\ K_I = \dfrac{K_p}{T_f}; \quad T_f = \dfrac{R_f}{L_f} \end{cases} \tag{19}$$

If the pole-zero cancellation method is used, the expressions of the parameters of the PI current controller can be expressed by (20) where τ_{BF} an imposed closed loop response time is optimising the system.

$$\begin{cases} K_p = \dfrac{L_f}{E_m}\sqrt{\dfrac{2}{3}}\dfrac{1}{\tau_{BF}} \\ K_I = \dfrac{R_f}{E_m}\sqrt{\dfrac{2}{3}}\dfrac{1}{\tau_{BF}} \end{cases} \tag{20}$$

III. SIMULATION RESULTS AND DISCUSSION

The simulation in this work has been developed in Matlab/Simulink environment.

Fig. 8 and fig. 9 give respectively the panel voltage and the output boost converter voltage where the DC voltage required by the inverter is chosen as a base value. The boost converter

voltage converges to the required one providing stepped-up voltage panel.

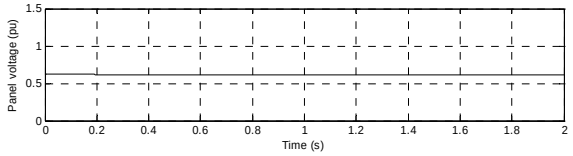

Fig. 8: Panel voltage response

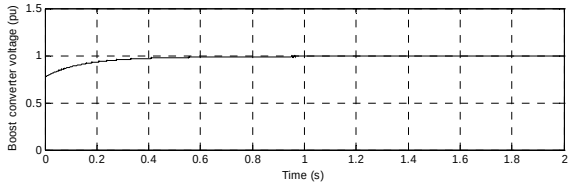

Fig. 9: Output boost converter voltage response.

The reference reactive power is equal to zero and the reference active power is equal to the nominal one. Fig. 10 and fig. 11 give reactive and the active power responses where the nominal power is used as base value. They converge to the references ones.

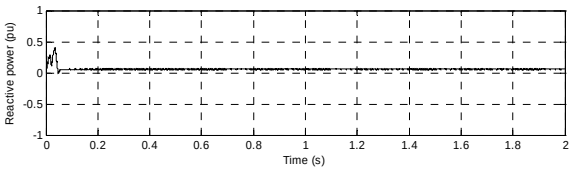

Fig. 10: Reactive power response

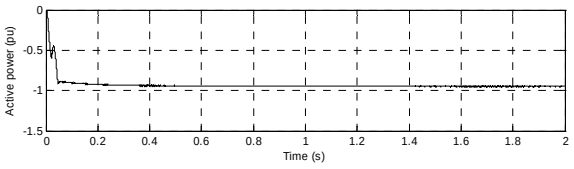

Fig. 11: Active power response

Fig. 12, fig. 13, and fig. 14 illustrate respectively the per phase grid per phase response, the per phase inverter connected grid voltage and the synchronisation frequency.

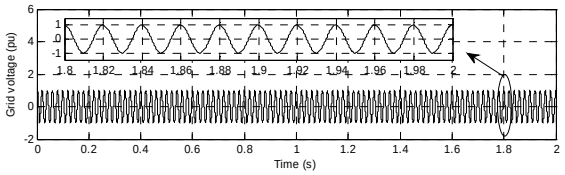

Fig. 12: Grid voltage response

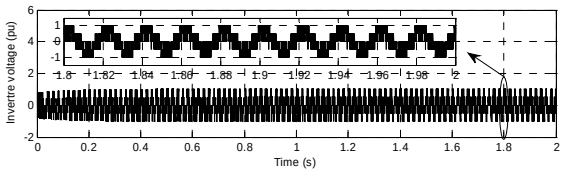

Fig. 13: Inverter voltage response

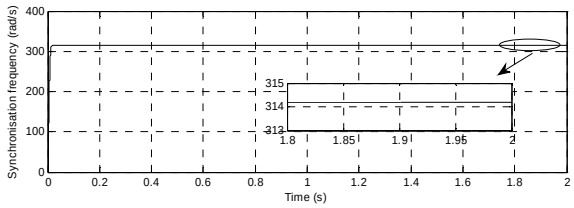

Fig. 14: Synchronisation frequency response

IV. CONCLUSION

The presented research work leads to the development of a controlled topology for a grid connected photovoltaic system.

Photovoltaic panel supplying a PMW controlled inverter grid connected has been found suitable for energy area application.

The boost converter provides a stepped-up voltage to the load when panel voltage stepped-up in order to adapt the required voltage load against insolation variation.

The power and the current control have been found suitable to perform the energy transfer.

Simulation results are presented high lighting the overall proposed good performances of the system. These promising results open the possibility for the reconstitution of the proposed scheme to be set up for an on-line implementation.

Appendix

TABLE I. PARAMETERS OF PV CELL (POLLY-CRYSTALLINE SILICON)

Open circuit voltage: V_{oc}	$0.6058\ V$
Short circuit current : I_{sc}	$8.1\ A$
Parallel cell's resistance: R_{pc}	$0.833\ \Omega$
Series cell's resistance: R_{sc}	$0.0833\ m\Omega$
Solar cell's ideal factor : k	1.450
reverse diode saturation current I_{rs}	$3.047e-7\ A$
Short circuit current temperature coefficient K_{SCT}	$1.73e-3A/°K$
Reference cell's temperature: T_{c_ref}	$25°C$
Boltzmann's constant: β	$1.38e-23$
Band gap energy: E_g	$1.11ev$

TABLE II. PARAMETERS OF PV MODULE

Rated output power	$216W$
Open circuit voltage: V_{oc}	$36.35\ V$
Number of series cells: n_s	60

TABLE III. PV ARRAY PARAMETERS

Open circuit voltage: V_{oc}	545 V
Short circuit current : I_{sc}	8.1 A
Number of series modules: N_s	6
Number of parallel modules: N_p	1

TABLE IV. GRID PARAMETERS

Rated voltage V_s	220 V
Grid resistance filter L_f	20 mH
Grid inductance filter R_f	5 Ω
Rated frequency ω_N	314 rad / s

REFERENCES

[1] M. Gaiceanu," Advanced State Feedback Control of Grid- Power Inverter,"Energy Procedia 14, pp.1464 – 1470, 2012

[2] S. H. Lee, S. G. Song, S. J. Park, C. J. Moon and M.H .Lee, "Grid-Connected photovoltaic system using current-source inverter," Solar Energy 82, pp. 411-419, 2008

[3] S.K . Kim , J.H. Jeon , C.H. Cho, E.S. Kim and J.B. Ahn," Modeling and simulation of a grid-connected PV generation system for electromagnetic transient analysis," Solar Energy 83, pp. 664-678, 2009.

[4] S. H. Lee, S. G. Song, S. J. Park, C. J. Moon and M.H .Lee ," Grid-Connected photovoltaic system using current-source inverter," Solar Energy 82, pp. 411-419, 2008.

[5] R. Chenni, M. Makhlouf, T. Kerbache, A. Bouzid, "A detailed modeling method for photovoltaic cells," Energy, vol.32, pp. 1724–1730, 2008.

[6] N. Hidouri , L. Sbita, "A New DTC-SPMSM Drive Scheme for PV Pumping System, International Journal of Systems Control," vol.1.3, pp. 113-121, 2010.

[7] N.Hidouri, T.Mhamdi, S.hammadi, L.Sbita, "A new hybrid photovoltaic-diesel system control scheme for an isolated load," IJRRAS, vo1.9, issue 2, pp. 270-281, 2011.

[8] N. Hidouri, S. Hammadi, L. Sbita, "An Advanced DPC-Self Excited Induction Generator Drive Scheme for an Isolated Wind turbine Boost System," International Review on Modelling and Simulations (IREMOS), vol. 5, No. 2, pp. 913-920, 2012.

[9] T. Bjazic, Z. Ban, I.Volaric, "Control of a Fuel Cell Stack loaded with DC/DC Boost Converter," Industrial Electronics. IEEE International Symposium, pp. 1489–1494, June 30-July.2, 2008.

[10] M. Monfared, S. Golestan," Control strategies for single-phase grid integration of small-scale renewable energy sources," Renewable and Sustainable Energy Reviews, vol.16, pp. 4982-4993, 2012

[11] A. Chaoui, J. Gauberta, F. Krim," Power quality improvement using DPC controlled three-phase shunt active filter," Electric Power Systems Research.80, pp. 657-666, 2010

[12] Y. Han , L. Xu , M. M. Khan a, G.Yao a, L.D. Zhou a, C. Chen ," A novel synchronization scheme for grid-connected converters by using adaptive linear optimal filter based PLL (ALOF PLL)," Simulation Modelling Practice and Theory, vol. 17 , pp. 1299–1345, 2009

[13] M. Monfared, S. Golestan," Control strategies for single-phase grid integration of small-scale renewable energy sources," Renewable and Sustainable Energy Reviews, vol.16, pp. 4982-4993, 2012.

[14] E. Pouresmaeil, O.G. Bellmunt, D.M. Miracle, J.B.Jané, " Multilevel converters control for renewable energy integration to the power grid", Energy 36 , pp. 950-963, 2011.

[15] E. Pouresmaeil, D. Montesinos-Miracle, Oriol Gomis-Bellmunt, Joan Bergas-Jané, "A multi-objective control strategy for grid connection of DG (distributed generation) resources", Energy35, pp. 5022-5030, 2010.

[16] M. Mohammadia,, M. Nafar, "Fuzzy sliding-mode based control (FSMC) approach of hybrid micro-grid in power distribution systems", Electrical Power and Energy Systems 51 , pp.232–242, 2013.

[17] R. Kadri, H. Andrei, J.P. Gaubert, T. Ivanovici, G. Champenois, P. Andre, "Modeling of the photovoltaic cell circuit parameters for optimum connection model and real-time emulator with partial shadow conditions", Energy 42, pp. 57-67, 2012.

[18] C.M. Hong, T.C. Ou, K.H. Lu, "Development of intelligent MPPT (maximum power point tracking) control for a grid-connected hybrid power generation system", Energy 50, pp. 270-279, 2013.

[19] A. Timbus, R. Teodorescu, P. Rodriguez, "Grid monitoring for distributed power generation systems to comply with grid codes", Proc. IEEE ISIE , pp.1608–1612.

[20] F. Ruza, A.Reyb, J.M. Torreloc, A. Nietob, F.J. Cánovasa, "Real time test benchmark design for photovoltaic grid-connected control systems", Electric Power System Research 81, pp.907-914, 2011.

[21] A. Chaoui, F. Krim, J. Gauberta, L. Rambault, " DPC controlled three-phase active filter for power quality improvement," Electric Power and energy Systems 30, pp. 467-485, 2008.

[22] Y. Han, L. Xu, M. M. Khan, G. Yao, L. D. Zhou, C. Chen," A novel synchronization scheme for grid-connected converters by using adaptive linear optimal filter based PLL (ALOF–PLL)", Simulation Modelling Practice and Theory 17 , pp. 1299–1345, 2009.

[23] M. Malinowski, G. Marques, M. Cichowlas, M. P. Kazmierkowski, "New Direct Power Control of Three-Phase PWM Boost Rectifiers under Distorted and Imbalanced Line Voltage Conditions". Conférence ISIE'03, vol. 1, pp.438-443, Juin 2003.

[24] A. Samadi, M. Ghandhari, L. Söder," Reactive Power Dynamic Assessment of a PV System in a Distribution Grid", Energy Procedia 20 , pp. 98 – 107 , 2012.